JACS
JOURNAL OF THE AMERICAN CHEMICAL SOCIETY
pubs.acs.org/JACS
Article

Chemical Kinetics and Mass Action in Coexisting Phases

Jonathan Bauermann,[#] Sudarshana Laha,[#] Patrick M. McCall, Frank Jülicher,[*] and Christoph A. Weber[*]

Cite This: J. Am. Chem. Soc. 2022, 144, 19294−19304
Read Online
ACCESS | Metrics & More | Article Recommendations | Supporting Information

ABSTRACT: The kinetics of chemical reactions are determined by the law of mass action, which has been successfully applied to homogeneous, dilute mixtures. At nondilute conditions, interactions among the components can give rise to coexisting phases, which can significantly alter the kinetics of chemical reactions. Here, we derive a theory for chemical reactions in coexisting phases at phase equilibrium. We show that phase equilibrium couples the rates of chemical reactions of components with their diffusive exchanges between the phases. Strikingly, the chemical relaxation kinetics can be represented as a flow along the phase equilibrium line in the phase diagram. A key finding of our theory is that differences in reaction rates between coexisting phases stem solely from phase-dependent reaction rate coefficients. Our theory is key to interpreting how concentration levels of reactive components in condensed phases control chemical reaction rates in synthetic and biological systems.

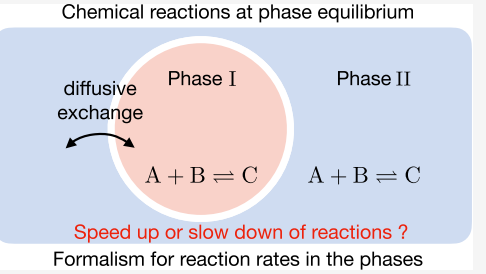

1. INTRODUCTION

The law of mass action sets the foundation for the kinetics of chemical reactions. It states that the rate of a reaction is proportional to the chemical activities of the reactants involved, where the chemical activity depends on concentrations. For a bimolecular reaction between the reactants A and B in a dilute, homogeneous solution, the reaction rate r is proportional to the concentrations of both reactants, $r \propto n_A n_B$. This proportionality arises because the encounters among reactants increase with the concentrations of both components.[1,2] For a reversible bimolecular reaction, A + B ⇌ C + D, chemical equilibrium corresponds to the balance of the forward and backward rates. At dilute conditions and chemical equilibrium, the law of mass action implies that the ratio of products to reactant equilibrium concentrations is constant, $K \equiv (n_C n_D)/(n_A n_B)$, where K is the equilibrium constant of the reaction and n_i are the concentrations of the reactive components, i = A, B, C, D.

The law of mass action also lays the foundation of reaction-diffusion models. Such models have been used to unravel the minimal principles underlying chemical patterns in nonliving[3,4] and living systems. Examples include pattern formation in tissues[5−7] or on artificial and cellular membranes.[8−12] In models of such systems, chemical reaction rates and diffusive fluxes are typically considered to be independent.[13]

However, the law of mass action needs to be carefully applied when mutual interactions among the components become important, particularly in nondilute solutions, where these interactions couple diffusion and chemical reactions. Such interactions can also give rise to phase separation, whereby the system demixes to form compositionally distinct coexisting phases. At phase equilibrium, all components in the coexisting phases have equal chemical potentials and equivalent equal chemical activities. Since chemical activities also determine chemical reactions, the condition of phase equilibrium is expected to govern chemical equilibrium[14,15] as well as chemical reaction kinetics in a way that differs from homogeneous solutions.

Recent experimental studies investigated the effects of coexisting phases on reversible and irreversible chemical reactions.[16−23] Increased[16] and decreased[17] reaction rates were reported inside condensed phases compared to their coexisting environment. Interestingly, an upconcentration of reactive components inside the condensed phase led to a decrease in reaction rates in some cases. It was suggested that this opposite trend is due to highly composition-dependent reaction rate coefficients.[17,18] To unravel the physiochemical principles underlying these experimental observations requires a theory of mass-action kinetics in phase-separated systems.

Here, we derive the kinetic theory for chemical reactions in coexisting phases that are at phase equilibrium. A key result of our work is that reaction rates are only different in two phases due to different reaction rate coefficients and not because of density differences leading to different frequencies of encounters among components. This result stems from the condition of phase equilibrium, which also implies a coupling between diffusion and chemical reaction kinetics due to molecular interactions. Phase equilibrium allows us to represent the relaxation kinetics of reactions as a chemical

Received: June 14, 2022
Published: October 14, 2022

https://doi.org/10.1021/jacs.2c06265
J. Am. Chem. Soc. 2022, 144, 19294−19304

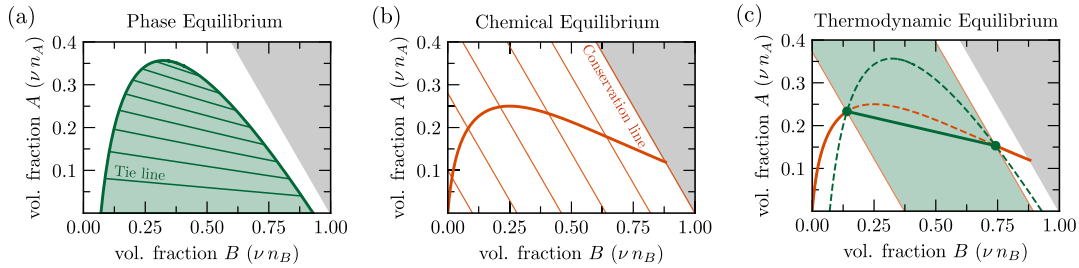

Figure 1. Equilibrium phase diagrams. To illustrate different equilibria, we consider a ternary, incompressible mixture composed of the components A, B, and a nonreactive solvent, with identical molecular volumes ν. (a) Phase equilibrium. Along the binodal line (thick green line), the phase equilibrium condition, eq 4, is fulfilled. Each coexisting pair of equilibrium volume fractions along the binodal line is connected by a tie line (thin green line). (b) Chemical equilibrium. Along the mononodal (thick orange line), the chemical equilibrium condition, eq 10, is satisfied. Chemical equilibrium for the reaction, A ⇌ B, corresponds to the intersection of the mononodal with a conservation line $\psi_1 = \nu(n_A + n_B)$ (thin orange line). (c) Thermodynamic equilibrium. In the case of a compatible phase and chemical equilibria, both equilibrium conditions (eqs 4 and 10) hold simultaneously. In this case, a single tie line is selected (thick green line), even for a broad range of conservation lines (green area). For incompatible equilibria, the system is homogeneous and compositions are determined by chemical equilibrium (thick orange line).

trajectory along the binodal manifold in the phase diagram. When chemical systems are maintained out of chemical equilibrium, we show that specific coexisting phases are selected, where reactive components are continuously exchanged between the phases at the steady state.

2. RESULTS AND DISCUSSION

2.1. Equilibria in Systems With Chemical Reactions and Coexisting Phases. To formulate the theory for chemical reactions in the coexisting phase, we first introduce the thermodynamic quantities and discuss the relevant equilibria of such systems. We emphasize that the following theory is general and can be applied to any type of chemical reaction network. In the following, we consider simple reactions of the type A ⇌ B and A + B ⇌ C for which we can visualize the kinetics in the phase diagrams. Furthermore, our theory can also be applied to any interactions among the components. To illustrate the interplay between phase separation and chemical reactions, we consider systems where only the product can phase separate.

2.1.1. Chemical Potential and Activity. For a solution composed of different types of chemical species C_i of molecular volumes ν_i ($i = 0, ..., M$), the chemical potential is defined as $\mu_i \equiv \partial G/\partial N_i|_{T,p,N_{j\neq i}}$, where $G(N_0, N_1, ..., N_M, p, T)$ is the Gibbs free energy (see Supporting Information, Section 1). Here, N_i denotes the particle number of chemical species C_i, where the index $i = 0$ corresponds to the solvent component, and $i = 1, ..., M$ indicates the solute components. The pressure is denoted by p, and T is the temperature. Introducing the concentrations $n_i = N_i/V$ with $V = \partial G/\partial p|_{T,N_i}$ denoting the system volume, we express the chemical potential in terms of the chemical activity a_i[24−27]

$$\mu_i(\{n_k\}, p, T) = \mu_i^0(p, T) + k_B T \log(a_i(\{n_k\}, p, T)) \tag{1}$$

where μ_i^0 is the reference chemical potential for $a_i = 1$, and $\{n_k\}$ denotes $n_0, n_1, ..., n_M$. The chemical activity

$$a_i(\{n_k\}, p, T) = \gamma_i(\{n_k\}, p, T)n_i \tag{2}$$

can be expressed in terms of the activity coefficients γ_i. If all solute components are sufficiently dilute with respect to the solvent component, all activity coefficients γ_i are positive constants. In contrast, in nondilute solutions, interactions among components imply that the activity coefficients γ_i depend on the concentrations of all components. Capturing interactions between components i and j by a mean-field energy density $\chi_{ij}N_iN_j/V^2$, where χ_{ij} is an interaction parameter, leads to an exponential dependence of the activity coefficient γ_i on all the concentrations n_j

$$\gamma_i = \nu_i \exp\left(\frac{\sum_{j=0}^{M}\chi_{ij}n_j - \nu_i S}{k_B T}\right) \tag{3}$$

with $S = k_B T \sum_{j=0}^{M} n_j + \sum_{j,k=0}^{M} \frac{\chi_{jk}}{2} n_j n_k$. Note that in the dilute limit the solvent volume fraction $n_0\nu_0 \simeq 1$, and all interactions involving solute components can be neglected, leading to a constant activity coefficient. The general form eq 3 of the activity coefficients is consistent with the Flory−Huggins model.[28,29] We will consider the activity coefficient shown in eq 3 to study how phase coexistence affects the kinetics of specific chemical reactions. Note that the corresponding results do not qualitatively depend on the specific form of activity coefficients related to a mean-field approximation.

2.1.2. Phase Equilibrium. Due to interactions among the components, nondilute solutions can separate into distinct coexisting phases of different compositions. Though we consider the coexistence of two phases I and II for simplicity, we stress that the theory developed below also applies to the coexistence of more than two phases. At phase equilibrium, pressures and temperatures are equal in each phase, $p^{\mathrm{I}} = p^{\mathrm{II}}$ and $T^{\mathrm{I}} = T^{\mathrm{II}}$. Also, the chemical potentials of each component i are in balance

$$\mu_i^{\mathrm{I}} = \mu_i^{\mathrm{II}} \tag{4}$$

These conditions are fulfilled by the equilibrium composition of the two coexisting phases with concentrations $n_i^{\mathrm{I/II}} = N_i^{\mathrm{I/II}}/V^{\mathrm{I/II}}$. Each pair of equilibrium concentrations, $\{n_k^{\mathrm{I}}\}$ and $\{n_k^{\mathrm{II}}\}$, are connected by a tie line. The collection of all such points makes up the binodal manifold in the phase diagram. For instance, Figure 1a depicts the phase diagram of an example of a ternary mixture. Equation 4 can be equivalently expressed as an equality of chemical activities in both phases

$$a_i^{\mathrm{I}} = a_i^{\mathrm{II}} \tag{5}$$

Molecular species partition unequally in the two phases, which is described by the partition coefficient of species i, defined as

https://doi.org/10.1021/jacs.2c06265
J. Am. Chem. Soc. 2022, 144, 19294−19304

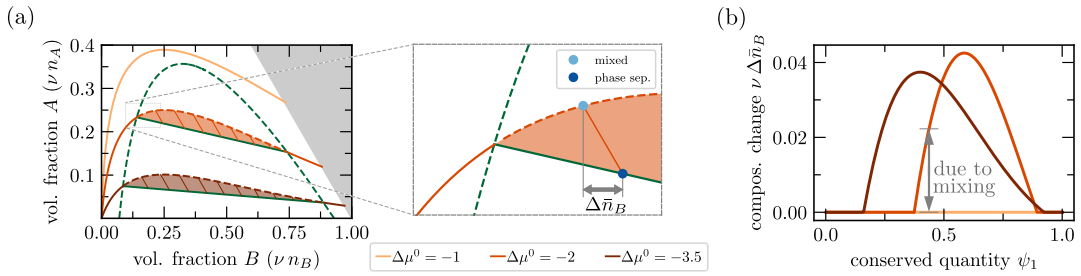

Figure 2. Phase separation controls chemical equilibrium. (a) Varying the difference of reference chemical potential between components B and A, $\Delta\mu^0$, leads to different chemical equilibrium lines (orange-colored mononodals) in the phase diagram. The orange lines in the shaded domains (see zoom-in) characterize the difference between the phase-separated system at thermodynamic equilibrium and the corresponding mixed system (gray arrow), indicating that phase separation can control chemical equilibrium. (b) This difference varies with the value of the conserved quantity ψ_1, which is depicted by the compositional change of the B-component, $\nu\Delta\bar{n}_B$, due to mixing.

$$P_i \equiv \frac{n_i^{\mathrm{I}}}{n_i^{\mathrm{II}}} \tag{6}$$

At phase equilibrium eq 4, the partition coefficients can be expressed in terms of the activity coefficients in both phases, $\gamma_i^{\mathrm{I/II}}$, by using eqs 1 and 2 as

$$P_i = \frac{\gamma_i^{\mathrm{II}}}{\gamma_i^{\mathrm{I}}} \tag{7}$$

This expression reveals that partitioning is governed by the composition dependence of activity coefficients $\gamma_i^{\mathrm{I/II}}$ in phase separating systems. If all solutes are dilute with respect to the solvent, solutes partition equally with $P_i = 1$ since there is no phase coexistence, that is, $\gamma_i^{\mathrm{I}} = \gamma_i^{\mathrm{II}}$. Note that the case $P_i = 1$ does not necessarily correspond to dilute solutes.

2.1.3. Chemical Equilibrium. We consider chemical reactions $\alpha = 1, \ldots, R$

$$\sum_{i=0}^{M} \sigma_{i\alpha}^{+} \mathrm{C}_i \rightleftharpoons \sum_{i=0}^{M} \sigma_{i\alpha}^{-} \mathrm{C}_i \tag{8}$$

of chemical species C_i, where $\sigma_{i\alpha}^{\pm}$ are stoichiometric matrices. In eq 8, reactants are on the left side, while reaction products are on the right side. Given $(M + 1)$ chemical species undergoing R linearly independent reactions, there exist $(M - R + 1)$ conserved quantities ψ_i, where $i = 0, \ldots, M - R$. The reaction Gibbs free energies corresponding to reaction α are

$$\Delta\mu_\alpha \equiv \sum_{i=0}^{M} \sigma_{i\alpha}\mu_i \tag{9}$$

where we abbreviate $\sigma_{i\alpha} = \sigma_{i\alpha}^{-} - \sigma_{i\alpha}^{+}$. The basis vectors spanning the nullspace of the matrix $\nu_i\sigma_{i\alpha}$ define linearly independent conserved quantities ψ_i.[30] The condition for chemical equilibrium reads

$$\Delta\mu_\alpha = 0 \tag{10}$$

At chemical equilibrium, the concentrations reach equilibrium values that can be used to define the equilibrium reaction coefficients as

$$K_\alpha \equiv \prod_{i=0}^{M} (n_i)^{\sigma_{i\alpha}} \tag{11}$$

which are distinct from the equilibrium reaction constants that include chemical activities instead of concentrations.[31]

At chemical equilibrium, eq 10, the equilibrium reaction coefficients K_α can be expressed in terms of the stoichiometric coefficients, activity coefficients, and reference chemical potentials as

$$K_\alpha = \prod_{i=0}^{M} \gamma_i^{-\sigma_{i\alpha}} \exp\left(-\frac{\sigma_{i\alpha}\mu_i^0}{k_{\mathrm{B}}T}\right) \tag{12}$$

The equilibrium reaction coefficients thus describe relationships between concentrations at chemical equilibrium. These coefficients depend on composition via the activity coefficients γ_i.[26,27] For dilute solutions, K_α is composition-independent and is thus often referred to as equilibrium reaction constants.

In general, for given conserved quantities of ψ_i, there exists a unique set of concentrations, n_i, that satisfy eq 11 and therefore correspond to chemical equilibrium. Figure 1b shows the example of a ternary mixture, where the conserved quantity, ψ_1, (see figure caption for definition) is constant along the thin straight lines (orange). The concentrations at chemical equilibrium lie on the intersection of a line with constant ψ_1 (thin orange line) with the line on which chemical equilibrium holds and eq 10 is satisfied (thick orange line). We refer to this line as mononodal since it describes a single set of equilibrated concentrations, while the binodal of phase separation characterizes pairs of equilibrated concentrations.

2.1.4. Thermodynamic Equilibrium. If a system is at thermodynamic equilibrium and two phases coexist, both chemical reactions and phases are equilibrated. In this case, eqs 10 and 4 are obeyed simultaneously. As a consequence, thermodynamic equilibrium imposes a relation between equilibrium reaction coefficients and partition coefficients. In fact, equilibrium reaction coefficients, K_α^{I} and K_α^{II}, differ in the two coexisting phases I and II. At thermodynamic equilibrium, their ratio obeys

$$\frac{K_\alpha^{\mathrm{I}}}{K_\alpha^{\mathrm{II}}} = \prod_{i=0}^{M} (P_i)^{\sigma_{i\alpha}} \tag{13}$$

This relationship between reaction coefficients and partition coefficients is a key result of our work since it connects chemical reactions and phase separation at thermodynamic equilibrium. Equation 13 can select a subset of coexisting concentrations on the binodal manifold if both equilibria are compatible. Combining the binodal and mononodal within one phase diagram represents a new concept that allows us to discuss how phase separation affects chemical reactions at equilibrium.

https://doi.org/10.1021/jacs.2c06265
J. Am. Chem. Soc. 2022, 144, 19294−19304

The case of compatible equilibria is illustrated in the example of a ternary mixture shown in Figure 1c, where a unique pair of concentrations coexist at thermodynamic equilibrium for a large range of conserved quantities (green circles). Chemical and phase equilibria can also be incompatible. In this case, thermodynamic equilibrium corresponds to a homogeneous state that satisfies only chemical equilibrium eq 10; top orange solid lines in Figure 2a.

An important implication of our concept to combine the binodal together with the mononodal in one phase diagram is that phase coexistence leads to different equilibrium states compared to the corresponding mixed system. To illustrate this effect, we compare the average composition $\overline{n}_i$ of a system at phase coexistence to the same system that is mixed but at chemical equilibrium. Mixing can be realized by stirring, for example. In the phase diagram, this comparison amounts to the deviation between the line of chemical equilibrium (dashed orange line in Figure 2a) and the tie line (solid green line in Figure 2a), which is depicted by the orange domains in Figure 2a.

Since the mixed case is only partially equilibrated, its composition is different from the composition at thermodynamic equilibrium. This difference varies with the value of the conserved quantity, ψ_1 (Figure 2b). This dependence on ψ_1 solely stems from mixing since for the considered ternary mixture with one chemical reaction at thermodynamic equilibrium, and changing the ψ_1 only affects the phase volumes and not the composition in each phase. The difference between the homogeneous, partially equilibrated state and the phase-separated, thermodynamic state reflects the influence of phase coexistence on chemical reactions.

2.2. Chemical Reaction Kinetics in Coexisting Phases at Phase Equilibrium. In this section, we study the kinetics of chemical reactions for systems composed of two homogeneous coexisting phases that are maintained at phase equilibrium but are not at chemical equilibrium. This condition of partial equilibrium holds when chemical reactions are slow compared to phase separation and corresponds to the case of reaction-limited chemical kinetics.[32,33] We will discuss the implications of our theory for systems that can relax toward chemical equilibrium and systems that are maintained away from equilibrium.

2.2.1. Kinetics of Concentrations and Phase Volumes. In each phase, the kinetics of the respective concentration of component i, $n_i^{\mathrm{I/II}}$ for $i = 0, ..., M$ is governed by (see Supporting Information, Section 2)

$$\frac{\mathrm{d}}{\mathrm{d}t}n_i^{\mathrm{I/II}} = r_i^{\mathrm{I/II}} - j_i^{\mathrm{I/II}} - \frac{n_i^{\mathrm{I/II}}}{V^{\mathrm{I/II}}}\frac{\mathrm{d}}{\mathrm{d}t}V^{\mathrm{I/II}} \tag{14a}$$

where $r_i^{\mathrm{I/II}}$ are the chemical reaction rates in the corresponding phases with phase volumes $V^{\mathrm{I/II}}$, and $j_i^{\mathrm{I/II}}$ are the diffusive exchange rates between phases. These rates maintain phase equilibrium at all times. Note that in this work, rates have the units of concentration per time. The last term of eq 14a accounts for changes in concentrations due to the changes of the respective phase volumes $V^{\mathrm{I/II}}$. The kinetics of these phase volumes follow (see Supporting Information, Section 2)

$$\frac{1}{V^{\mathrm{I/II}}}\frac{\mathrm{d}}{\mathrm{d}t}V^{\mathrm{I/II}} = \sum_{i=0}^{M}\nu_i^{\mathrm{I/II}}(r_i^{\mathrm{I/II}} - j_i^{\mathrm{I/II}}) + \sum_{i=0}^{M} n_i^{\mathrm{I/II}}\frac{\mathrm{d}}{\mathrm{d}t}\nu_i^{\mathrm{I/II}} \tag{14b}$$

where $\nu_i^{\mathrm{I/II}}$ denote the phase-dependent molecular volumes. If the molecular volumes $\nu_i = \nu_i(p, T)$ are only functions of pressure p and temperature T and are not dependent on composition, then they are equal in both phases at isobaric and isothermal conditions and therefore $\mathrm{d}\nu_i^{\mathrm{I/II}}/\mathrm{d}t = 0$. For volume conserving reactions with $\sum_{i=0}^{M}\sigma_{i\alpha}\nu_i = 0$, it follows that $\sum_{i=0}^{M}\nu_i r_i^{\mathrm{I/II}} = 0$ for each reaction α.

2.2.2. Diffusive Exchange Rates between Phases. To maintain phase equilibrium while chemical reactions occur, components need to be exchanged between the phases. This exchange conserves the total number of components in the system, which implies that for the diffusive exchange rates $j_i^{\mathrm{I/II}}$

$$V^{\mathrm{I}}j_i^{\mathrm{I}} = -V^{\mathrm{II}}j_i^{\mathrm{II}} \tag{15}$$

As a result, for systems with composition-independent molecular volumes and volume-conserving reactions, the total system volume $V = V^{\mathrm{I}} + V^{\mathrm{II}}$ is constant with respect to time (see eq 14b).

The condition of phase equilibrium (eq 5) at all times during the reaction kinetics implies that

$$\frac{\mathrm{d}}{\mathrm{d}t}(\gamma_i^{\mathrm{I}}n_i^{\mathrm{I}}) = \frac{\mathrm{d}}{\mathrm{d}t}(\gamma_i^{\mathrm{II}}n_i^{\mathrm{II}}) \tag{16}$$

Using eqs 14a and 14b in eq 16 together with eq 15 gives a set of $2(M + 1)$ equations that are linear in the diffusive exchange rates $j_i^{\mathrm{I/II}}$. Therefore, the diffusive exchange rates can be written in closed-form expressions $j_i^{\mathrm{I/II}}(\{r_k^{\mathrm{I}}, r_k^{\mathrm{II}}\}, V^{\mathrm{I}}, V^{\mathrm{II}})$, which depend only on the chemical reaction rates, $r_k^{\mathrm{I/II}}$, and the phase volumes, $V^{\mathrm{I/II}}$.

2.2.3. Reaction Rates at Phase Equilibrium. The chemical reaction rate of each component, in eq 14a can be written in terms of the net reaction rate, $r_\alpha^{\mathrm{I/II}}$, of the reaction α in each of the phases as

$$r_i^{\mathrm{I/II}} = \sum_{\alpha=1}^{R}\sigma_{i\alpha}r_\alpha^{\mathrm{I/II}} \tag{17}$$

This net reaction rate can be split into the forward (+) and the backward (−) reaction rates, i.e., as $r_\alpha = r_\alpha^+ - r_\alpha^-$.

The condition for thermodynamic equilibrium implies that the relationships, $r_\alpha^+ = r_\alpha^-$ and $j_i^{\mathrm{I/II}} = 0$ hold simultaneously in all phases. The forward and backward rates in both phases obey a detailed balance of the rates

$$\frac{r_\alpha^+}{r_\alpha^-} = \exp\left(-\frac{\Delta\mu_\alpha}{k_{\mathrm{B}}T}\right) \tag{18}$$

with the reaction free energy $\Delta\mu_\alpha$ given by eq 9. Equation 18 is fulfilled by choosing the forward and the backward rates as

$$r_\alpha^\pm = k_\alpha(\{n_k\}, p, T)\exp\left(\frac{\sum_{i=0}^{M}\sigma_{i\alpha}^\pm\mu_i}{k_{\mathrm{B}}T}\right) \tag{19}$$

Here, $k_\alpha(\{n_k\}, p, T)$ denotes a reaction rate coefficient that depends on temperature, pressure, and composition $\{n_k\}$. Note that thermodynamics does not determine the value of the reaction rate coefficient. Rather, it only constrains the coefficient to be positive and thereby guarantees that the entropy of the system increases.

Using eq 19, the chemical reaction rate of component i (eq 17) can be written as

https://doi.org/10.1021/jacs.2c06265
J. Am. Chem. Soc. 2022, 144, 19294−19304

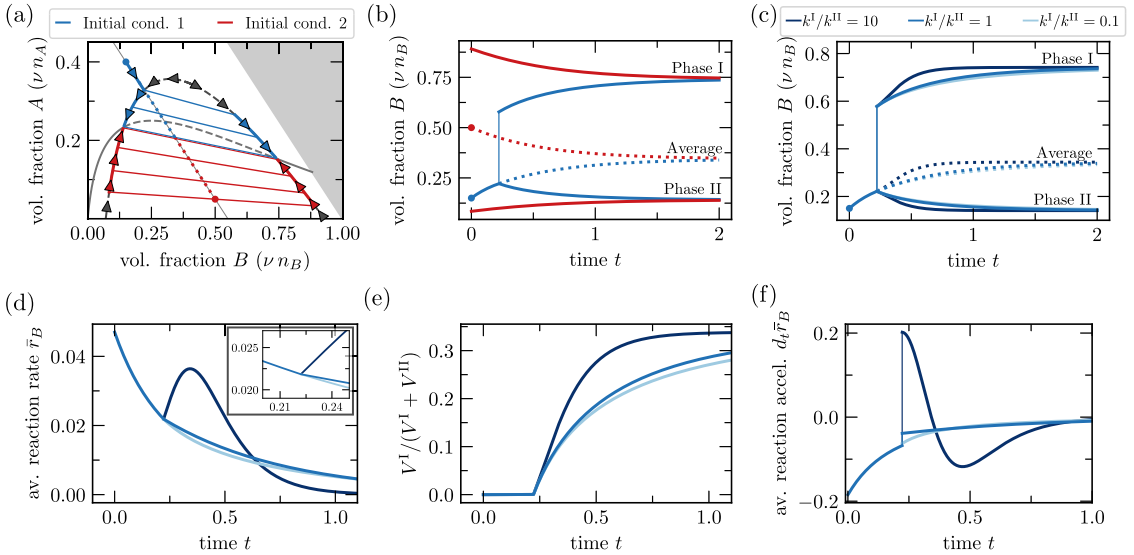

Figure 3. Kinetics of a unimolecular reaction relaxing to thermodynamic equilibrium. We consider the kinetics of a ternary, incompressible mixture and the chemical reaction eq 26. (a) Different choices of initial conditions 1 (blue) and 2 (red) follow different flow fields. However, both initial conditions lead to the same thermodynamic equilibrium because they lie on the same conserved line $\psi_1 = 0.55$; see also (b) showing the chemical trajectories for product B, where solid and dotted lines correspond to volume fraction in phase I/II and averages, respectively. (c) Difference in reaction rate coefficients between two phases affects reaction rates (in both phases and average) but not the thermodynamic equilibrium state. The average volume fraction of product B changes continuously at the onset of phase separation for initial condition 1. The average reaction rate of product B, $\overline{r}_B$ (d), and the phase fraction, V^I/V (e), has a kink at the onset of phase separation, implying that (f) average reaction acceleration of product B, $d\overline{r}_B/dt$, jumps at the onset of phase separation. Please note that the kink and the jump require that phase equilibrium is established quasi-instantaneously on the time scales of chemical reactions.

$$r_i^{\mathrm{I/II}} = \sum_{\alpha=1}^{R} k_\alpha^{\mathrm{I/II}} \sigma_{i\alpha} H_\alpha \tag{20}$$

where we introduce the chemical reaction force

$$H_\alpha = \exp\left(\frac{\mu_\alpha^+}{k_B T}\right) - \exp\left(\frac{\mu_\alpha^-}{k_B T}\right) \tag{21}$$

Here, we have also introduced the reactant (+) and product (−) free energies $\mu_\alpha^\pm$ via

$$\Delta\mu_\alpha = \mu_\alpha^- - \mu_\alpha^+ \tag{22}$$

Equations 14a and 14b together with the phase equilibrium conditions eq 16 and the chemical reaction rates, described by eqs 20 and 21, govern the kinetics of chemical reactions at phase equilibrium. These kinetic equations represent a key result of our work since they extend the chemical laws for dilute and homogeneous systems with reactions[24,26,34] to nondilute and phase-separated systems.

2.2.4. Chemical Reactions Relaxing to Chemical Equilibrium. For systems that can relax to thermodynamic equilibrium, the reactant and product free energies are directly determined by the chemical potentials

$$\mu_\alpha^\pm = \sum_{i=0}^{M} \sigma_{i\alpha}^\pm \mu_i \tag{23}$$

and the chemical reaction force can thus be expressed in terms of the chemical activities as

$$H_\alpha = \prod_{m=0}^{M} \left(e^{\mu_m^0/k_B T} a_m\right)^{\sigma_{m\alpha}^+} - \prod_{m=0}^{M} \left(e^{\mu_m^0/k_B T} a_m\right)^{\sigma_{m\alpha}^-} \tag{24}$$

This form of the chemical reaction force is specific to systems that can relax to thermodynamic equilibrium and implies various properties for chemical reactions occurring at phase equilibrium.

2.2.5. Key Properties of Chemical Reactions at Phase Equilibrium. First, at phase equilibrium, the chemical activities $a_i = \gamma_i n_i$ are equal in both phases. For chemical reactions that can relax to thermodynamic equilibrium, equal chemical activities between the phases imply that the chemical reaction forces H_α (eq 21) are equal in both phases as well. Note that the reaction forces are equal despite the composition difference between the phases. This key result of our work emerges because chemical activities (or equivalently chemical potentials) govern both the chemical kinetics of the components in the phases and their diffusion between the phases. Equal reaction forces H_α between phases imply that the chemical reaction rate $r_i^{\mathrm{I/II}}$ of component i shown in eq 20 is different between the phases only due to the composition-dependent reaction rate coefficients $k_\alpha^{\mathrm{I/II}}$.

Second, due to phase equilibrium, the rate of change of the concentration of a reactive molecule in one of the phases, $dn_i^{\mathrm{I/II}}/dt$, is not equal to the chemical reaction rate $r_i^{\mathrm{I/II}}$ of the component. The reason is that, in addition, the diffusive exchange of reactive components between the phases $j_i^{\mathrm{I/II}}$ and changes in phase volumes $dV^{\mathrm{I/II}}/dt$ contribute to concentration changes in each phase; see eq 14a. Both contributions are crucial since they maintain phase equilibrium during the chemical kinetics, that is, the concentrations $n_i^{\mathrm{I/II}}$ remain on the binodal manifold which is defined by the condition for phase equilibrium (eq 4). Thus, the determination of reaction rates in each phase requires the knowledge of both the diffusive exchange rates between the phases and how the phase volumes change with time.

https://doi.org/10.1021/jacs.2c06265
J. Am. Chem. Soc. 2022, 144, 19294−19304

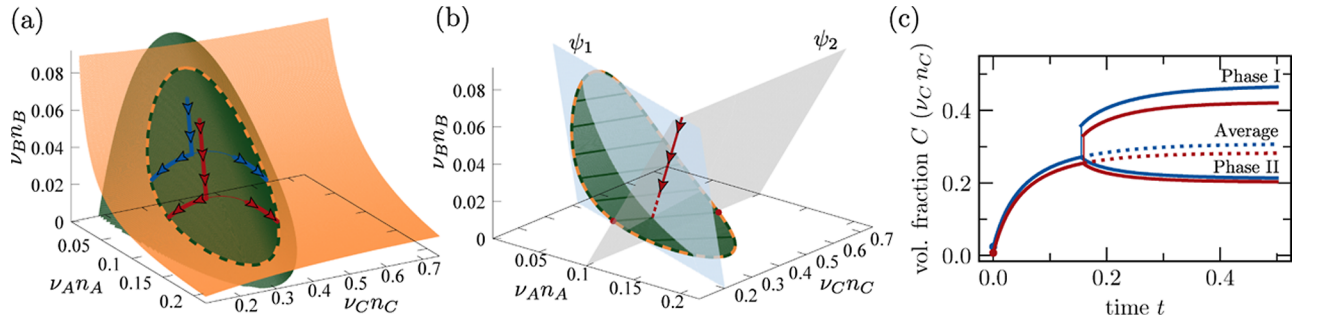

Figure 4. Kinetics of a bimolecular reaction relaxing to thermodynamic equilibrium. We illustrate the kinetics of a quaternary, incompressible mixture and the chemical reaction eq 27. (a) Phase equilibrium and chemical equilibrium are represented by two surfaces (green and orange, respectively). The closed line given by the intersection of these two surfaces depicts the thermodynamic equilibria states (dashed green line). The solid blue and red lines correspond to trajectories of two systems with different values of conserved quantities (see (b)). We have chosen $\psi_1 = 0.42$ with $\psi_2 = 0.05$ for the blue trajectory and $\psi_2 = 0.1$ for the red trajectory. (b) Two planes of conserved quantities defined by ψ_1 (light blue plane) and ψ_2 (gray plane) intersect to uniquely define a line (solid red as in (a)) along which the trajectory of the average volume fractions progresses during kinetics. At the intersection of this unique line with the manifold of thermodynamic equilibrium, the compositions in each phase (red dots) are also uniquely selected. (c) Chemical trajectories for product C, where solid and dotted lines correspond to volume fractions in phase I/II and averages, respectively for two systems (red and blue). The volume fractions in each phase and average, therefore, evolve to different thermodynamic equilibrium states.

Third, the chemical kinetics at phase equilibrium differs from the kinetics of the corresponding mixed system. We already discussed in Figure 2a,b that the thermodynamic state is distinct from the corresponding well-mixed system. In contrast to such well-mixed systems where the chemical kinetics is governed by the composition of the mixture, the chemical kinetics at phase equilibrium is determined by the chemical activities (or chemical potentials) along the binodal manifold together with the phase-dependent reaction rate coefficients. This difference can be illustrated when, for example, considering the kinetics of the average concentrations, $\overline{n}_i = (V^{\mathrm{I}} n_i^{\mathrm{I}} + V^{\mathrm{II}} n_i^{\mathrm{II}})/V$. Using eqs 14a and 14b, the corresponding kinetics is given by

$$\frac{\mathrm{d}\overline{n}_i}{\mathrm{d}t} = \sum_{\alpha=1}^{R} \left(\frac{V^{\mathrm{I}}}{V} k_\alpha^{\mathrm{I}} + \frac{V^{\mathrm{II}}}{V} k_\alpha^{\mathrm{II}} \right) \sigma_{i\alpha} H_\alpha \tag{25}$$

for volume-conserving reactions. We find that in systems with coexisting phases I and II, the time evolution of the average composition is determined by the kinetics of the phase volumes $V^{\mathrm{I/II}}$, the phase-dependent reaction rate coefficients $k_\alpha^{\mathrm{I/II}}$, and the phase-independent reaction force H_α.

2.2.6. Unimolecular Chemical Reactions in Coexisting Phases. In this section, we discuss an example of a ternary mixture with chemically reactive components A and B and a nonreactive solvent S. For simplicity, we assume identical molecular volume ν for all components. We consider a single reaction whereby solute A can spontaneously convert to product B and vice versa without the participation of any additional components, referred to as an unimolecular chemical reaction

$$\mathrm{A} \rightleftharpoons \mathrm{B} \tag{26}$$

Note that for systems that chemically react via unimolecular reactions and that can phase separate, the chemical reaction rates of components eq 20 are generally nonlinear in the solute concentrations. For such a unimolecular reaction in a ternary mixture, we can define two conserved quantities, $\psi_1 = \nu(n_{\mathrm{A}} + n_{\mathrm{B}})$ and $\psi_0 = \nu n_{\mathrm{S}}$. We numerically solve the governing kinetic equations of the unimolecular chemical reaction eq 26 at phase equilibrium; for details see Supporting Information, Section 3.

The kinetics of a unimolecular chemical reaction at phase equilibrium can be illustrated as a chemical trajectory in a simple phase diagram spanned by two reactive components A and B (Figure 3a). For an initial composition within the binodal (red dot in Figure 3a), the concentrations in each phase follow a flow field along the binodal lines (solid red lines in Figure 3a). The corresponding average composition moves along the conservation line of fixed ψ_1 while crossing different tie lines (dotted red line in Figure 3a). Changes in tie line as the chemical reaction proceeds imply corresponding compositional changes in the coexisting phases. For an initial composition outside the binodal (blue dot in Figure 3a), the initially well-mixed system moves along the conservation line and the phase separates into coexisting phases when the composition reaches the binodal line (solid blue lines in Figure 3a). The onset of phase separation leads to a discontinuity of the volume fractions, which otherwise evolve smoothly over time (Figure 3b). Then, similar to the previous initial condition, the phase composition follows the flow along the binodal lines. Since both cases are identical except for their initial conditions, both relax to the same thermodynamic equilibrium state.

Varying the reaction rate coefficients $k_\alpha^{\mathrm{I/II}}$ in the phases can strongly alter the chemical kinetics (Figure 3c). When the reaction rate coefficient is increased in the B product-rich phase ($k_\alpha^{\mathrm{I}}/k_\alpha^{\mathrm{II}} = 10$), product B relaxes more quickly toward thermodynamic equilibrium. The same holds true for the average concentration of product B. Interestingly, at the onset of phase separation, the average reaction rate $\overline{r}_i = (V^{\mathrm{I}} r_i^{\mathrm{I}} + V^{\mathrm{II}} r_i^{\mathrm{II}})/V$ (rhs. of eq 25) is continuous but can kink for reaction rate coefficients that are unequal between the phases ($k_\alpha^{\mathrm{I}} \neq k_\alpha^{\mathrm{II}}$); see Figure 3d and inset for average reaction rate of product B, $\overline{r}_{\mathrm{B}}$. Average reaction rate $\overline{r}_{\mathrm{B}}$ can even initially increase before relaxing to thermodynamic equilibrium ($\overline{r}_{\mathrm{B}} = 0$). This increase is a result of an initial very fast growth of phase I, which stems from the fast formation of product B in phase I (Figure 3e).

The kink of the average reaction rate $\overline{r}_{\mathrm{B}}$ at the onset of phase separation implies a jump in the acceleration of the chemical reaction, $\mathrm{d}\overline{r}_{\mathrm{B}}/\mathrm{d}t$ (Figure 3f). In other words, as coexisting phases form, there is a drastic change in the average reaction

https://doi.org/10.1021/jacs.2c06265
J. Am. Chem. Soc. 2022, 144, 19294−19304

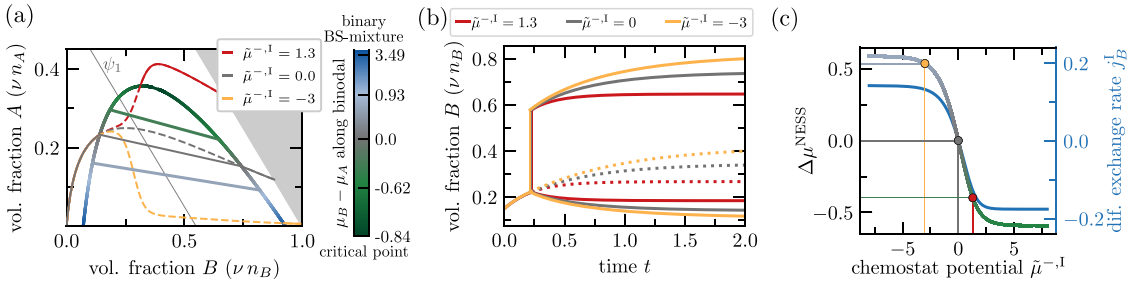

Figure 5. Unimolecular chemical reaction maintained away from chemical equilibrium. (a) Depending on the value of the chemostat potential $\tilde{\mu}^{-,\mathrm{I}}$, different coexisting phases are selected (green tie line for $\tilde{\mu}^{-,\mathrm{I}} = 1.3$ and light blue -gray line for $\tilde{\mu}^{-,\mathrm{I}} = -3.0$). The color bar represents the chemical potential difference between the components B and A along the binodal line, where the lower/upper bound corresponds to the critical point/binary B/S mixture. (b) Chemical trajectories for product B, where solid and dotted lines correspond to volume fractions in phase I/II and averages, respectively. Chemical kinetics and nonequilibrium steady states vary with the value of the chemostat potential, $\tilde{\mu}^{-,\mathrm{I}}$. (c) More the chemostat potential, $\tilde{\mu}^{-,\mathrm{I}}$, deviates from zero, the more the system is maintained away from thermodynamic equilibrium. The nonequilibrium steady state is characterized by the nonequilibrium reaction free energy, $\Delta\mu^{\mathrm{NESS}}$. The gray dot corresponds to the reference system at thermodynamic equilibrium, while the red and orange dots represent the two nonequilibrium steady states depicted in (a,b). Diffusive exchange rate j_B^{I} at the NESS (blue curve with the corresponding axis at the r.h.s.) is nonzero as the system is maintained away from thermodynamic equilibrium via the chemostat potential $\tilde{\mu}^{-,\mathrm{I}}$. Results in (a,b,c) are obtained for $\psi_1 = 0.55$.

rate of the system. This change reflects the effect of phase separation on the kinetics of chemical reactions.

2.2.7. Bimolecular Chemical Reactions in Coexisting Phases. As a further example of a chemically reactive system at phase equilibrium, we study a four-component system that contains three reactive solutes i = A, B, C and a nonreactive solvent S. In this example, the solutes undergo a bimolecular chemical reaction

$$\mathrm{A} + \mathrm{B} \rightleftharpoons \mathrm{C} \tag{27}$$

which conserves volume (see Supporting Information, Section 3B for details). For such a bimolecular chemical reaction in a four-component mixture, there exist three conserved quantities. Each conserved quantity is represented by a plane in a three-dimensional phase diagram spanned by the volume fractions of the reactive solute components A, B, C. The three conserved quantities are $\psi_0 = \nu_S n_S$, $\psi_1 = \nu_A n_A + \nu_B n_B + \nu_C n_C$, and $\psi_2 = \nu_A n_A - \nu_B n_B$, and the intersection of the planes corresponding to conserved quantities ψ_1 and ψ_2 yields a line in the phase diagram.

The chemical kinetics of a bimolecular reaction at phase equilibrium can be depicted as a chemical trajectory in the three-dimensional phase diagram. Figure 4a shows two chemical trajectories corresponding to systems with two different values of conserved quantities. For both cases, the kinetics of the average composition follows the intersection of the respective conserved planes, ψ_1 and ψ_2, which is illustrated for one initial condition in Figure 4b. As phase separation occurs, the volume fractions in each phase move along the binodal surface (green). The chemical kinetics stop when the volume fractions in the coexisting phases reach the thermodynamic equilibrium (green-orange dashed line in Figure 4a,b). The thermodynamic equilibria lie on a closed line and are given by the intersection between the binodal surface and the chemical equilibrium surface with the condition, $\mu_A + \mu_B = \mu_C$. Concomitantly, the volume fraction of product C saturates (red and blue lines in Figure 4c). These saturation values differ since the thermodynamic equilibrium state depends on the conserved quantities (shown by the tie lines in Figure 4b).

2.2.8. Chemical Reactions Maintained away from Chemical Equilibrium. Chemical reactions can also be maintained away from thermodynamic equilibrium. This is common in living cells, where biochemical reactions are chemically driven by the consumption of a chemical fuel.[35,36] Maintaining reactions away from chemical equilibrium can lead to nonequilibrium steady states (NESS) with nonvanishing diffusive exchange rates between the phases.

Here, we consider systems at phase equilibrium that are maintained away from chemical equilibrium. This can, for example, be realized by coupling the system to a chemical fuel and its reaction products that are maintained at fixed chemical potentials. If the chemical reaction α can take place with and without coupling to the fuel, we can define an effective reaction free energy

$$\Delta\mu_\alpha = \sum_{i=0}^{M} \sigma_{i\alpha}\mu_i + \Delta\tilde{\mu}_\alpha \tag{28}$$

where the external reaction free energy $\Delta\tilde{\mu}_\alpha$ describes the contribution stemming from the fuel reservoir (see Supporting Information, Section 4). Following eq 22, we can also express the effective reaction free energy $\Delta\mu_\alpha$ as the difference between effective reactant (+) and product (−) free energies

$$\mu_\alpha^{\pm} = \sum_{i=0}^{M} \sigma_{i\alpha}^{\pm}\mu_i + \tilde{\mu}_\alpha^{\pm} \tag{29}$$

where $\tilde{\mu}_\alpha^{\pm}$ are external the reactant and product free energies that can be set by a chemostat. If the external reaction free energy $\Delta\tilde{\mu}_\alpha \neq 0$, NESSs can occur. Note that in certain cases, equilibrium states can be reached even if $\Delta\tilde{\mu}_\alpha \neq 0$. Specifically, this happens when $\Delta\tilde{\mu}_\alpha$ can be written as $\Delta\tilde{\mu}_\alpha = \sum_{i=0}^{M}\sigma_{i\alpha}c_i$, where the c_i are constants for each component, i, but are equal in the phases and for all reactions α. If c_i were different for different reactions, reaction equilibrium could not be reached.[37−39] If they were different for different phases, phase equilibrium could not be reached. If these conditions are not satisfied, the system cannot settle into thermodynamic equilibrium. Here, we focus on systems where the coupling to chemostats leads to a composition-dependent external reaction free energy $\Delta\tilde{\mu}_\alpha$ in the presence of coexisting phases. In this case, phase and chemical equilibrium cannot be fulfilled at the same time.

The incompatibility of phase and chemical equilibrium can be seen in the phase diagram looking at the intersection points

https://doi.org/10.1021/jacs.2c06265
J. Am. Chem. Soc. 2022, 144, 19294−19304

of the binodal manifold with the effective chemical equilibrium manifold, $\Delta\mu_\alpha = 0$ (e.g., yellow and red lines in Figure 5a). These intersection points cannot be connected by a tie line. Therefore, there can be NESSs, where $dn_i^{I/II}/dt = 0$ and $dV^{I/II}/dt = 0$ but reaction rates $r_i^{I/II}$ and diffusive exchange rates $j_i^{I/II}$ are non-zero, respectively.

A measure of the deviation of chemical reaction α from thermodynamic equilibrium can be defined as

$$\Delta\mu_\alpha^{NESS} \equiv \sum_{i=0}^{M} \sigma_{i\alpha}\mu_i^{NESS} \tag{30}$$

where μ_i^{NESS} are steady state chemical potentials. The quantity $\Delta\mu_\alpha^{NESS}$ is the original reaction free energy given by eq 9 but determined in the nonequilibrium state. Since μ_i^{NESS} are identical in the two phases due to phase equilibrium, the nonequilibrium reaction free energy

$$\Delta\mu_\alpha^{NESS}/k_BT = \log\left(\frac{k_\alpha^I V^I \exp\left(\frac{\tilde{\mu}_\alpha^{+,I}}{k_BT}\right) + k_\alpha^{II} V^{II} \exp\left(\frac{\tilde{\mu}_\alpha^{+,II}}{k_BT}\right)}{k_\alpha^I V^I \exp\left(\frac{\tilde{\mu}_\alpha^{-,I}}{k_BT}\right) + k_\alpha^{II} V^{II} \exp\left(\frac{\tilde{\mu}_\alpha^{-,II}}{k_BT}\right)}\right) \tag{31}$$

is phase independent. Equation 31 results from the balance of reaction and diffusive exchange rates $r_i^{I/II} = j_i^{I/II}$, which corresponds to the steady state condition of eq 14a together with $dV^{I/II}/dt = 0$. The nonequilibrium reaction free energies, $\Delta\mu_\alpha^{NESS}$, can be interpreted as the response of the system to external reactant and product free energies $\tilde{\mu}_\alpha^{\pm,I/II}$ that are set by a chemostat. The values of the nonequilibrium reaction free energies are dependent on the reaction rate coefficients $k_\alpha^{I/II}$ and the phase volumes at the steady state, $V^{I/II}$.

To illustrate the kinetics of chemical reactions and steady states that are maintained away from chemical equilibrium but are at phase equilibrium, we study the same unimolecular reaction in a ternary mixture as in Section 2.2.6. To maintain the reaction away from chemical equilibrium, we choose a nonzero external product free energy $\tilde{\mu}^{-,I}$, which we also refer to as chemostat potential. For simplicity, the other external reactant and product free energies $\tilde{\mu}^{\pm,II}$ and $\tilde{\mu}^{+,I}$ are chosen to be zero. Therefore, the effective chemical equilibrium line, $\Delta\mu = 0$, is only affected in phase I (solid red and yellow lines compared to the gray line in Figure 5a. For a single reaction, however, a NESS can only be reached in systems with coexisting phases.

For such systems, an important finding is that by choosing different values of the chemostat potential $\tilde{\mu}^{-,I}$, the chemical kinetics change and the system relaxes to different NESSs. For each value of $\tilde{\mu}^{-,I}$, such steady states have specific compositions in the coexisting phases indicating that the chemical driving can select distinct states of the chemically reactive system (solid green and light blue, respectively, in Figure 5a,b). Moreover, the chemical trajectories of the volume fractions in each phase (solid lines) and the average volume fractions (dotted lines) change when varying the chemostat potential $\tilde{\mu}^{-,I}$; see Figure 5b. In particular, the jump of the average acceleration $d\overline{r_i}/dt$ is also affected by the external reaction free energy (not shown).

The reaction free energy in the NESS $\Delta\mu^{NESS}$ is used to characterize how much the considered system deviates from thermodynamic equilibrium for a given value of the chemostat potential $\tilde{\mu}^{-,I}$. Around thermodynamic equilibrium, $\tilde{\mu}^{-,I}$ varies linearly, while for large deviations, $\Delta\mu^{NESS}$ saturates at two plateaus depending on the sign of the chemostat potential $\tilde{\mu}^{-,I}$ (Figure 5c). In particular, large and positive $\tilde{\mu}^{-,I}$ favor the conversion from component B to A in phase I. This trend is opposed by a decrease in the volume of phase I, therefore leading to the plateau for such values of $\tilde{\mu}^{-,I}$. Consistent with this, the value of the plateau of $\Delta\mu^{NESS}$ is determined by the volume of phase I, which is in turn set by the conserved quantity ψ_1. Specifically, the plateau value corresponds to the intersection of the line of conserved quantity ψ_1 (thin gray line) and the binodal line; see Figure 5a. In contrast, small and negative values of $\tilde{\mu}^{-,I}$ favor the conversion from component A to B in phase I. The full conversion is not possible since chemical reactions are only maintained away from chemical equilibrium in phase I, and thus the volume of phase I limits the selection of coexisting NESSs.

For chemically driven systems, the phase volumes are strongly influenced by an external supply of reaction free energy. This property is distinct from chemically driven systems since, at thermodynamic equilibrium, the phase volumes are solely determined by the conserved quantity. In particular, a ternary mixture with one chemical reaction at thermodynamic equilibrium becomes an effective binary mixture of two conserved quantities. As a result, varying these conserved quantities solely changes the phase volumes (Figure 1c). In contrast, for a chemically driven system, changing the conserved quantities also affects phase composition (see Supporting Information, Section 5).

3. CONCLUSIONS

In our work, we developed a theory of the chemical kinetics in phase-separated mixtures at phase equilibrium. For simplicity, we considered the case of homogeneous phases which arises when chemical reactions are slow compared to the phase separation kinetics. This includes systems where chemical reactions are rate limiting, such as reactions with biological enzymes.[32] This separation of time scales implies that the size of each phase is smaller than the reaction-diffusion length scales, which are set by the reaction rate coefficients and the diffusion coefficients. If these conditions are satisfied, we can consider the case of chemical reactions in coexisting phases that are each homogeneous and well-mixed.

For systems with chemical reactions that are slow compared to the phase separation kinetics, we showed that the condition of phase equilibrium governs chemical equilibrium. Therefore, chemical equilibrium in coexisting phases differs from the chemical equilibrium where all components are well mixed. Furthermore, the kinetics of reactions approaching chemical equilibrium also differs between phase-separated and the corresponding well-mixed system. We show that in a phase-separated system, the relaxation kinetics can be represented by a chemical trajectory of time-dependent phase concentrations that move along the binodal manifold in the phase diagram. We also find that conservation laws play an important role in phase-separated systems. Quantities conserved by the reactions define manifolds in composition space to which average compositions are confined. Such conservation manifolds, together with the manifolds of chemical and phase equilibria, govern the combined kinetics of reactions and phase separation.

Phase separation organizing chemical reactions was suggested as an important concept to understand cellular biochemistry.[40−43] In particular, phase-separated condensates can provide distinct biochemical environments and serve to

https://doi.org/10.1021/jacs.2c06265
J. Am. Chem. Soc. 2022, 144, 19294−19304

localize and confine chemical reactions.[44,45] The study of biochemical processes in phase-separated systems is currently a rapidly growing field. Our theory can play an important role to interpret observations in experimental systems where solute components undergo chemical reactions in the presence of coexisting phases. In particular, our work clarifies that the increased concentration of reactants in a condensed phase does not by itself lead to increased reaction rates. Rather, if the coexisting phases are at phase equilibrium, the reaction rates $r_i^{\mathrm{I/II}}$ of component i in each phase can only differ due to different reaction rate coefficients, $k_\alpha^{\mathrm{I/II}}$. In other words, the increased local concentration of a reactive solute due to phase separation does not necessarily increase the rates of reactions in which it participates. The speed-up or slow-down of reactions is solely determined by the reaction rate coefficients in each phase, which can also decrease upon condensation. These insights might be relevant to explain recent observations in coacervate emulsions with enzymatic reactions.[17,46−48] According to our theory, the reaction rate coefficients $k^{\mathrm{I/II}}$ can be determined by measuring the rate of concentration changes, $\dot{n}_i^{\mathrm{I/II}}$ (eqs 14a and 14b), together with the diffusive exchange rates between the phases and potential volume changes of coacervates. Another important insight of our work is that the rate of change of the concentration of reactive molecule i in one phase is not equal to the chemical reaction rate, $r_i^{\mathrm{I/II}}$, of this component. This is because phases are coupled and components are rapidly exchanged between the phases at phase equilibrium. To determine the chemical reaction rate $r_i^{\mathrm{I/II}}$ of component i, the diffusive exchange rate between the phases as well as the changes in phase volumes need to be taken into account. Thus, the chemical kinetics in coexisting phases tightly integrates phase separation kinetics and reaction kinetics. To highlight this point, we note that the effect of phase separation on chemical reactions in two coexisting phases cannot be inferred from the study of reactions in the two phases when they are isolated.

We also discussed chemical reactions at phase equilibrium but maintained away from chemical equilibrium via an external supply of free energy. Such external free energy could, for instance, be supplied via a chemical fuel. We find that the resulting nonequilibrium steady states (NESSs) have nonzero chemical reaction rates and nonzero diffusive exchange rates of components between the phases. At the NESSs, both of these nonzero rates balance each other. We showed that the steady-state concentrations in the two phases depend on the external reaction free energy. Thus, controlling the external reaction free energy supply can be used to select distinct compositions of coexisting phases and to vary the phase volumes. For systems maintained away from chemical equilibrium, the chemical reaction rates $r_i^{\mathrm{I/II}}$ can be phase dependent due to the supply of external free energy, which can differ between the phases, in addition to phase-dependent reaction rate coefficients $k^{\mathrm{I/II}}$. Thus, for such driven systems, reaction rates in the two phases can be controlled externally, even allowing opposite net directions of chemical reactions between the phases.

Using equations for the chemical kinetics of dilute, homogeneous mixtures for systems that can phase separate is incorrect if the system can relax toward thermodynamic equilibrium. First, there are diffusive exchanges between the phases that cannot be ignored. Second, systems that phase separate are nondilute and have chemical activities that are nonlinear in concentrations, which govern the kinetics of the chemical reaction, in particular at concentrations where mixtures can phase separate. For instance, in phase-separated systems, unimolecular reactions cannot be described as first-order reactions when the system can relax toward thermodynamic equilibrium. Applying equations for the chemical kinetics of dilute, homogeneous mixtures to phase-separated systems would implicitly correspond to a driven system with a supply of external free energy.

The results of our work could be tested in experimental systems such as coacervates with enzymatic reactions.[17,49−52] It will be interesting to compare chemically reactive systems at phase equilibrium with their well-mixed counterparts. In our theory, we considered that equilibration is quasi-instantaneous among the co-existing phases and at the interfaces. Thus, an interesting extension of our work is to account for the effects of the interface on chemical reactions. In particular, reactive solute components at the interfaces could show complex kinetics due to interfacial effects such as effective resistance,[53−55] thereby altering the transport between the coexisting phases.

■ ASSOCIATED CONTENT

Supporting Information

The Supporting Information is available free of charge at https://pubs.acs.org/doi/10.1021/jacs.2c06265.

Gibbs free energy density for the multicomponent mixture and a derivation of the kinetic equations starting from the extensive thermodynamic quantities of particle numbers and phase volumes; physio-chemical parameters used for numerical computations and externally maintaining chemical reactions away from equilibrium; and condition which selects the NESS for different values of the conserved quantity for ternary systems (PDF)

■ AUTHOR INFORMATION

Corresponding Authors

Frank Jülicher − *Max Planck Institute for the Physics of Complex Systems, 01187 Dresden, Germany; Center for Systems Biology Dresden, 01307 Dresden, Germany; Cluster of Excellence Physics of Life, TU Dresden, 01062 Dresden, Germany*; Email: julicher@pks.mpg.de

Christoph A. Weber − *Faculty of Mathematics, Natural Sciences, and Materials Engineering: Institute of Physics, University of Augsburg, 86159 Augsburg, Germany*; orcid.org/0000-0001-6279-0405; Email: christoph.weber@physik.uni-augsburg.de

Authors

Jonathan Bauermann − *Max Planck Institute for the Physics of Complex Systems, 01187 Dresden, Germany; Center for Systems Biology Dresden, 01307 Dresden, Germany*; orcid.org/0000-0002-0301-7655

Sudarshana Laha − *Max Planck Institute for the Physics of Complex Systems, 01187 Dresden, Germany; Center for Systems Biology Dresden, 01307 Dresden, Germany*; orcid.org/0000-0001-8256-0850

Patrick M. McCall − *Max Planck Institute for the Physics of Complex Systems, 01187 Dresden, Germany; Center for Systems Biology Dresden, 01307 Dresden, Germany; Max Planck Institute of Molecular Cell Biology and Genetics,*

01307 Dresden, Germany; orcid.org/0000-0002-6623-4673

Complete contact information is available at: https://pubs.acs.org/10.1021/jacs.2c06265

Author Contributions

#J.B. and S.L. contributed equally to this work.

Notes

The authors declare no competing financial interest.

■ ACKNOWLEDGMENTS

We thank Stefano Bo, Giacomo Bartolucci, and Tyler Harmon for insightful discussions. We kindly thank Evan Spruijt for providing helpful references on the history of the law of mass action. F.J. acknowledges funding from the Volkswagen Foundation. C.A.W. acknowledges the European Research Council (ERC) under the European Union's Horizon 2020 research and innovation programme ("Fuelled Life" with Grant agreement no. 949021) for financial support.

■ REFERENCES

(1) Benson, S. W. *The Foundations of Chemical Kinetics*; McGraw-Hill Book Co.: New York, NY, 1960.
(2) Christov, S. G. *Collision Theory and Statistical Theory of Chemical Reactions*; Springer, 1980.
(3) Castets, V.; Dulos, E.; Boissonade, J.; De Kepper, P. Experimental evidence of a sustained standing turing-type non-equilibrium chemical pattern. *Phys. Rev. Lett.* **1990**, *64*, 2953−2956.
(4) Horváth, J.; Szalai, I.; De Kepper, P. An experimental design method leading to chemical turing patterns. *Science* **2009**, *324*, 772−775.
(5) Turing, A. M. *The Chemical Basis of Morphogenesis*; Philosophical Transactions of the Royal Society of London; Series B, Biological Sciences, 1952; Vol. *237*(641), pp 37−72.
(6) Asai, R.; Taguchi, E.; Kume, Y.; Saito, M.; Kondo, S. Zebrafish leopard gene as a component of the putative reaction-diffusion system. *Mech. Dev.* **1999**, *89*, 87−92.
(7) Meinhardt, H. *Models of Biological Pattern Formation*; Academic Press: London, 1982.
(8) Loose, M.; Fischer-Friedrich, E.; Ries, R.; Kruse, K.; Schwille, P. Spatial regulators for bacterial cell division self-organize into surface waves in vitro. *Science* **2008**, *320*, 789−792.
(9) Goehring, N. W.; Trong, P. K.; Bois, J. S.; Chowdhury, D.; Nicola, E. M.; Hyman, A. A.; Grill, S. W. Polarization of par proteins by advective triggering of a pattern-forming system. *Science* **2011**, *334*, 1137−1141.
(10) Halatek, J.; Frey, E. Rethinking pattern formation in reaction−diffusion systems. *Nat. Phys.* **2018**, *14*, 507−514.
(11) Hubatsch, L.; Peglion, F.; Reich, J. D.; Rodrigues, N. T. L.; Hirani, N.; Illukkumbura, R.; Goehring, N. W. A cell-size threshold limits cell polarity and asymmetric division potential. *Nat. Phys.* **2019**, *15*, 1078−1085.
(12) Ramm, B.; Heermann, T.; Schwille, P. The e. coli mincde system in the regulation of protein patterns and gradients. *Cell. Mol. Life Sci.* **2019**, *76*, 4245−4273.
(13) Kondo, S.; Miura, T. Reaction-diffusion model as a framework for understanding biological pattern formation. *Science* **2010**, *329*, 1616−1620.
(14) Seyboldt, R. The dynamics of chemically active droplets, PhD Thesis, Technische Universität Dresden, 2019.
(15) Arana, O. A. Chemical control of liquid phase separation in the cell. PhD Thesis, Technische Universität Dresden, 2019.
(16) Strulson, C. A.; Molden, R. C.; Keating, C. D.; Bevilacqua, P. C. Rna catalysis through compartmentalization. *Nat. Chem.* **2012**, *4*, 941−946.
(17) Drobot, B.; Iglesias-Artola, M.; Le Vay, K.; Mayr, K.; Kar, V.; Kreysing, M.; Mutschler, M.; Tang, H.; Tang, T.-Y. D. Compartmentalised rna catalysis in membrane-free coacervate protocells. *Nat. Commun.* **2018**, *9*, 3643.
(18) Nakashima, K. K.; Vibhute, M. A.; Spruijt, E. Biomolecular chemistry in liquid phase separated compartments. *Front. Mol. Biosci.* **2019**, *6*, 21.
(19) Donau, C.; Späth, F.; Sosson, M.; Kriebisch, B. A. K.; Schnitter, F.; Tena-Solsona, M.; Kang, H.-S.; Salibi, E.; Sattler, M.; Mutschler, H.; Boekhoven, B. Active coacervate droplets as a model for membraneless organelles and protocells. *Nat. Commun.* **2020**, *11*, 5167.
(20) Schwarz, P. S.; Laha, S.; Janssen, J.; Huss, T.; Boekhoven, J.; Weber, C. A. Parasitic behavior in competing chemically fueled reaction cycles. *Chem. Sci.* **2021**, *12*, 7554−7560.
(21) Testa, A.; Dindo, M.; Rebane, A. A.; Nasouri, B.; Style, R. W.; Golestanian, R.; Dufresne, E. R.; Laurino, P. Sustained enzymatic activity and flow in crowded protein droplets. *Nat. Commun.* **2021**, *12*, 6293.
(22) Kueffner, A. M.; Linsenmeier, M.; et al. Sequestration within biomolecular condensates inhibits abeta 42 amyloid formation. *Chem. Sci.* **2021**, *12*, 4373−4382.
(23) Peeples, W.; Rosen, M. K. Mechanistic dissection of increased enzymatic rate in a phase-separated compartment. *Nat. Chem. Biol.* **2021**, *17*, 693−702.
(24) Alberty, R. A. *Thermodynamics of Biochemical Reactions*; Wiley-Interscience: Hoboken, N.J, 2003.
(25) Burgot, J.-L. *The Notion of Activity in Chemistry*; Springer International Publishing, 2017.
(26) Atkins, P.; Jones, L. *Chemical Principles: The Quest for Insight*; W.H. Freeman, 2009.
(27) Adam, G.; Läuger, P.; Stark, G. . *Physikalische Chemie und Biophysik*; Springer-Verlag Berlin Heidelberg, 2009.
(28) Flory, P. J. Thermodynamics of high polymer solutions. *J. Chem. Phys.* **1942**, *10*, 51−61.
(29) Huggins, M. L. Some properties of solutions of long-chain compounds. *J. Phys. Chem.* **1942**, *46*, 151−158.
(30) Palsson, B. *Systems Biology: Properties of Reconstructed Networks*; Cambridge University Press: Cambridge ; New York, 2006.
(31) Lewis, G. N. Outlines of a new system of thermodynamic chemistry. *Proc. Am. Acad. Arts Sci* **1907**, *43*, 259−293.
(32) Bar-Even, A.; Noor, E.; Savir, Y.; Liebermeister, W.; Davidi, D.; Tawfik, D. S.; Milo, R. The moderately efficient enzyme: Evolutionary and physicochemical trends shaping enzyme parameters. *Biochemistry* **2011**, *50*, 4402−4410.
(33) Milo, R.; Philips, R. *Cell Biology by the Numbers*; CRC Press, 2015.
(34) Denbigh, K. *The Principles of Chemical Equilibrium*; Cambridge University Press: Cambridge, 1961.
(35) Patel, A.; Malinovska, L.; Saha, S.; Wang, J.; Alberti, S.; Krishnan, Y.; Hyman, A. ATP as a biological hydrotrope. *Science* **2017**, *356*, 753−756.
(36) Babl, B.; Giacomelli, G.; Ramm, B.; Gelmroth, A.-K.; Bramkamp, M.; Schwille, P. Ctp-controlled liquid−liquid phase separation of parb. *J. Mol. Biol.* **2022**, *434*, 167401.
(37) Beard, D. A.; Liang, S. dan; Qian, H. Energy balance for analysis of complex metabolic networks. *Biophys. J.* **2002**, *83*, 79−86.
(38) Hill, T. L. *Free Energy Transduction and Biochemical Cycle Kinetics*; Springer-Verlag: New York, 1989.
(39) Rao, R.; Esposito, M. Nonequilibrium thermodynamics of chemical reaction networks: Wisdom from stochastic thermodynamics. *Phys. Rev. X* **2016**, *6*, 041064.
(40) Alberti, S. Phase separation in biology. *Curr. Biol.* **2017**, *27*, R1097−R1102.
(41) Banani, S. F.; Lee, H. O.; Hyman, A. A.; Rosen, M. K. Biomolecular condensates: organizers of cellular biochemistry. *Nat. Rev. Mol. Cell Biol.* **2017**, *18*, 285−298.
(42) Shin, Y.; Brangwynne, C. P. Liquid phase condensation in cell physiology and disease. *Science* **2017**, *357*, No. eaaf4382.

(43) Weber, C. A.; Zechner, C. Drops in cells. *Phys. Today* **2021**, *74*, 38−43.
(44) Su, X.; Ditlev, J. A.; Hui, E.; Xing, W.; Banjade, S.; Okrut, O.; King, D. S.; Taunton, T.; Rosen, M. K.; Vale, R. D. Phase separation of signaling molecules promotes t cell receptor signal transduction. *Science* **2016**, *352*, 595−599.
(45) Sheu-Gruttadauria, J.; MacRae, I. J. Phase transitions in the assembly and function of human mirisc. *Cell* **2018**, *173*, 946−957 e16.
(46) Koga, S.; Williams, D. S.; Perriman, A. W.; Mann, S. Peptide-nucleotide microdroplets as a step towards a membrane-free protocell model. *Nat. Chem.* **2011**, *3*, 720−724.
(47) Kojima, T.; Takayama, S. Membraneless compartmentalization facilitates enzymatic cascade reactions and reduces substrate inhibition. *ACS Appl. Mater. Interfaces* **2018**, *10*, 32782−32791.
(48) Stroberg, W.; Schnell, S. Do cellular condensates accelerate biochemical reactions? lessons from microdroplet chemistry. *Biophys. J.* **2018**, *115*, 3−8.
(49) Love, C.; Steinkühler, S.; Gonzales, D. T.; Yandrapalli, N.; Robinson, T.; Dimova, R.; Tang, T. Y. Reversible ph-responsive coacervate formation in lipid vesicles activates dormant enzymatic reactions. *Angew. Chem., Int. Ed.* **2020**, *59*, 5950−5957.
(50) Nakashima, K. K.; Baaij, J. F.; Spruijt, E. Reversible generation of coacervate droplets in an enzymatic network. *Soft Matter* **2018**, *14*, 361−367.
(51) Altenburg, W. J.; Yewdall, N. A.; Vervoort, D. F. M.; van Stevendaal, M. H. E.; Mason, A. F.; van Hest, J. C. M. Programmed spatial organization of biomacromolecules into discrete, coacervate-based protocells. *Nat. Commun.* **2020**, *11*, 6282.
(52) Chen, Y.; Yuan, M.; Zhang, Y.; Liu, S.; Yang, X.; Wang, K.; Liu, J. Construction of coacervate-in-coacervate multi-compartment protocells for spatial organization of enzymatic reactions. *Chem. Sci.* **2020**, *11*, 8617−8625.
(53) Taylor, N. O.; Wei, M.-T.; Stone, H. A.; Brangwynne, C. P. Quantifying dynamics in phase-separated condensates using fluorescence recovery after photobleaching. *Biophys. J.* **2019**, *117*, 1285−1300.
(54) Hahn, T.; Münchow, G. .; Hardt, S. Electrophoretic transport of biomolecules across liquid-liquid interfaces. *J. Phys.: Condens. Matter* **2011**, *23*, 184107.
(55) Gebhard, F.; Hartmann, J.; Hardt, S. Interaction of proteins with phase boundaries in aqueous two-phase systems under electric fields. *Soft Matter* **2021**, *17*, 3929−3936.

https://doi.org/10.1021/jacs.2c06265
J. Am. Chem. Soc. 2022, 144, 19294−19304